



Supplement of

Laser-Induced Fluorescence coupled with Machine Learning as an effective approach for real-time identification of bacteria in bioaerosols

Alejandro Fontal et al.

Correspondence to: Alejandro Fontal (alejandro.fontal@isglobal.org)

The copyright of individual parts of the supplement might differ from the article licence.

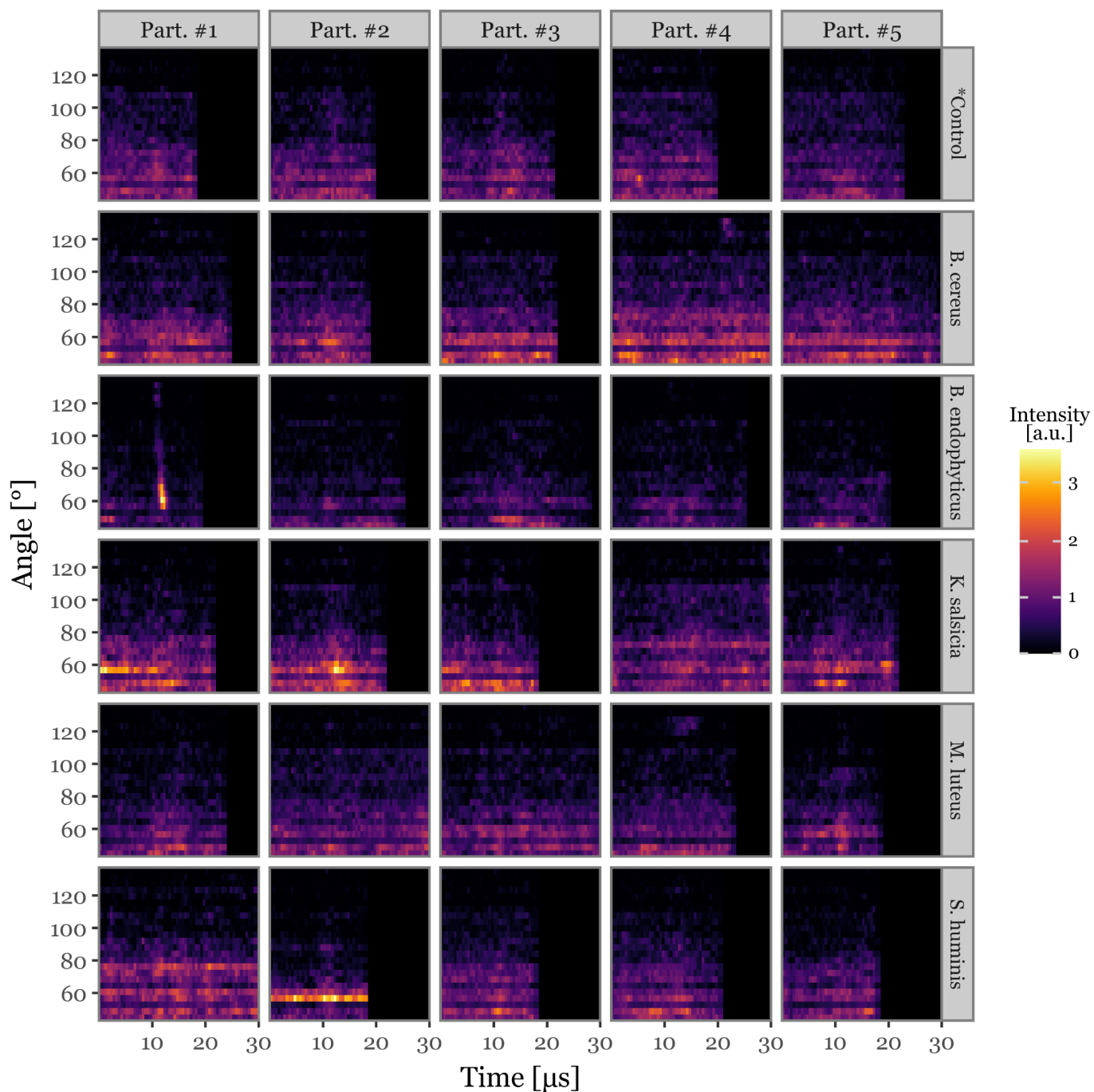


Figure S1. Example of the scattering images of 5 particles per sample group as they are either cropped or zero padded to 60 acquisitions (30 μ s time) to be included in the models.

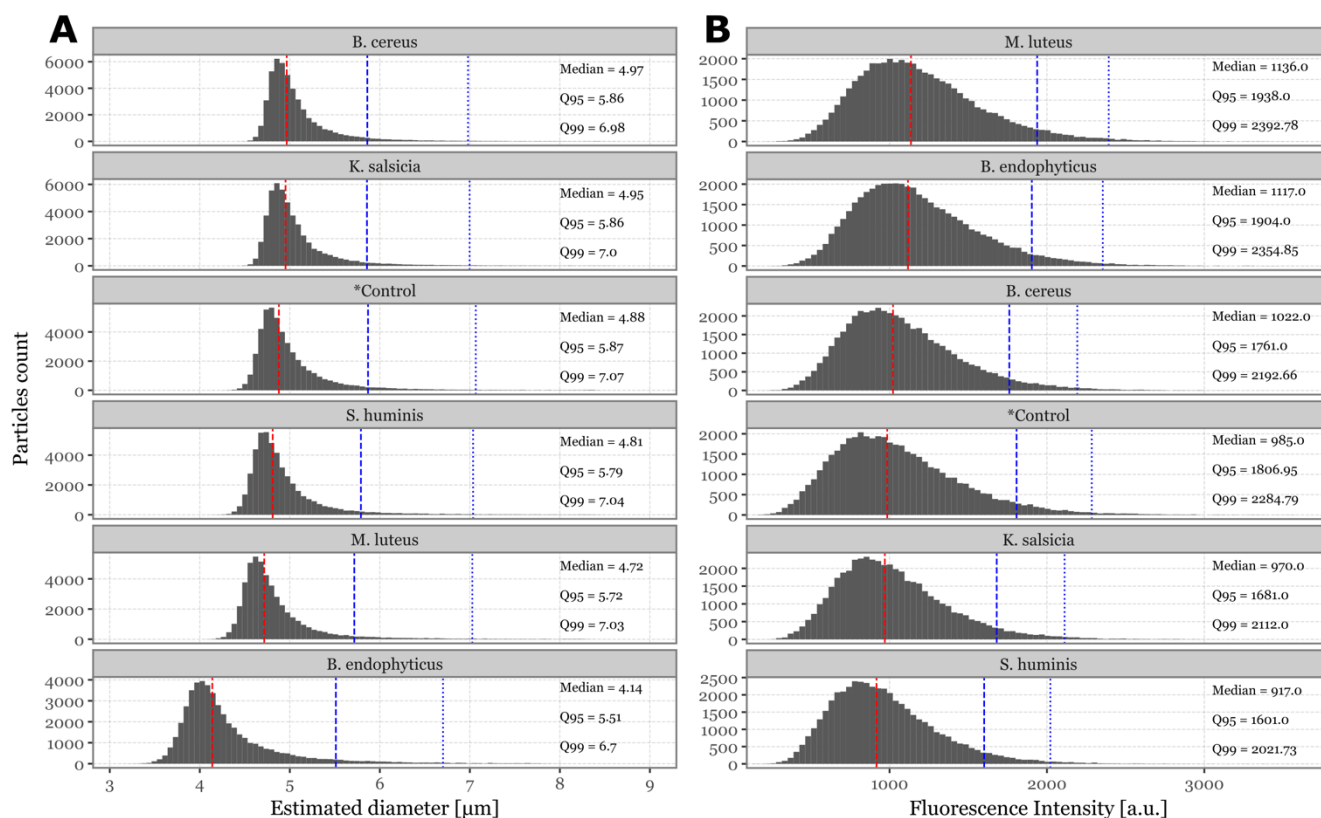


Figure S2. Size and fluorescence intensity distribution for bacterial samples. Panel A (left) depicts the distributions of estimated diameters per sample group, and panel B (right) depicts the distribution of maximum recorded fluorescence intensities per sample group. Red vertical line indicates the median, with the blue dashed line indicating the 95th percentile and the blue dotted line indicating the 99th percentile.

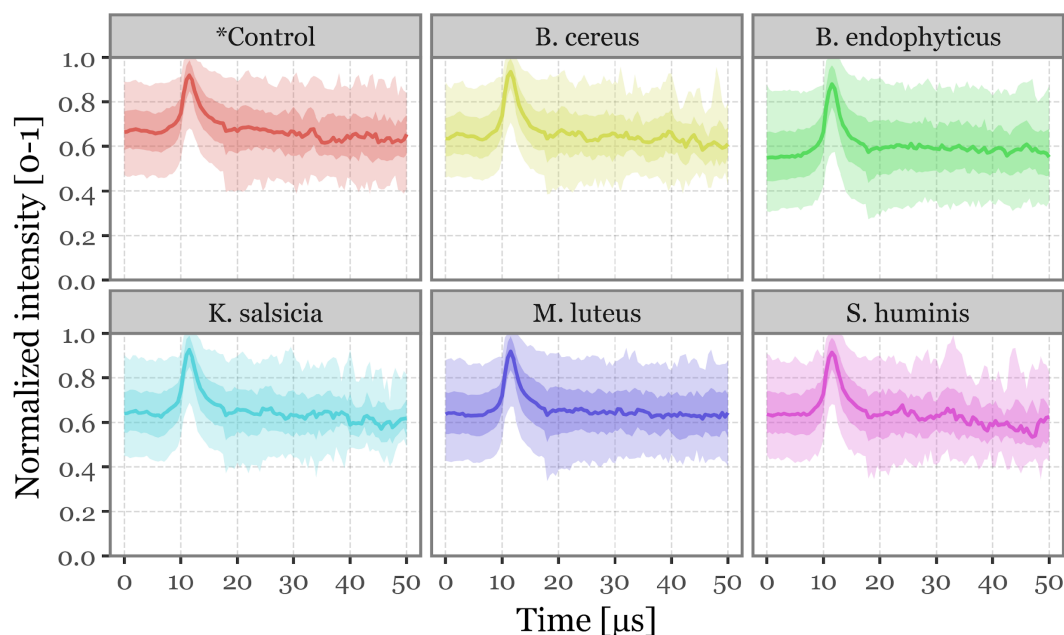


Figure S3. Distribution of scattering intensity across all angles as a function of acquisition time. The solid line represents the median value for all particles within each group. The darker shaded area indicates the interquartile range (25th to 75th), while the lighter shaded area represents the 5th to 95th percentile range.

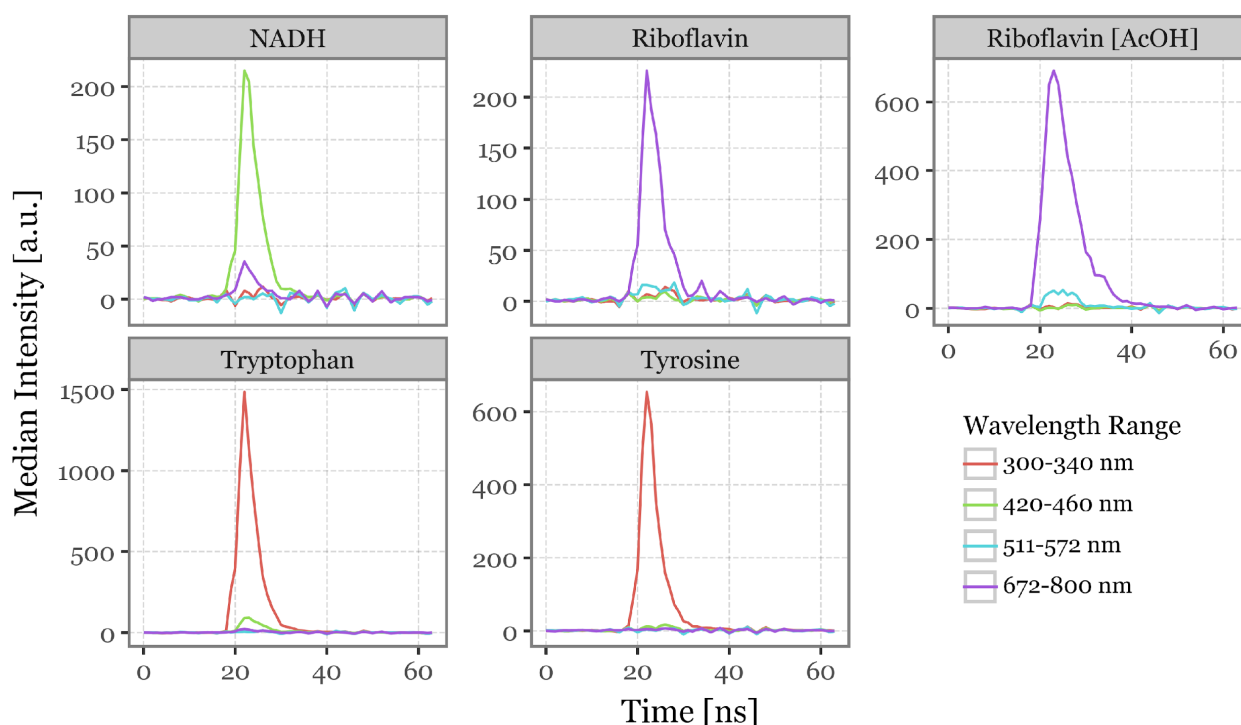


Figure S4. Fluorescence lifetimes for aerosolized fluorophores. Median fluorescence intensity as a function of time (in ns) for the 4 specified wavelength ranges across the 100 most fluorescent particles for each of the aerosolized fluorophores.

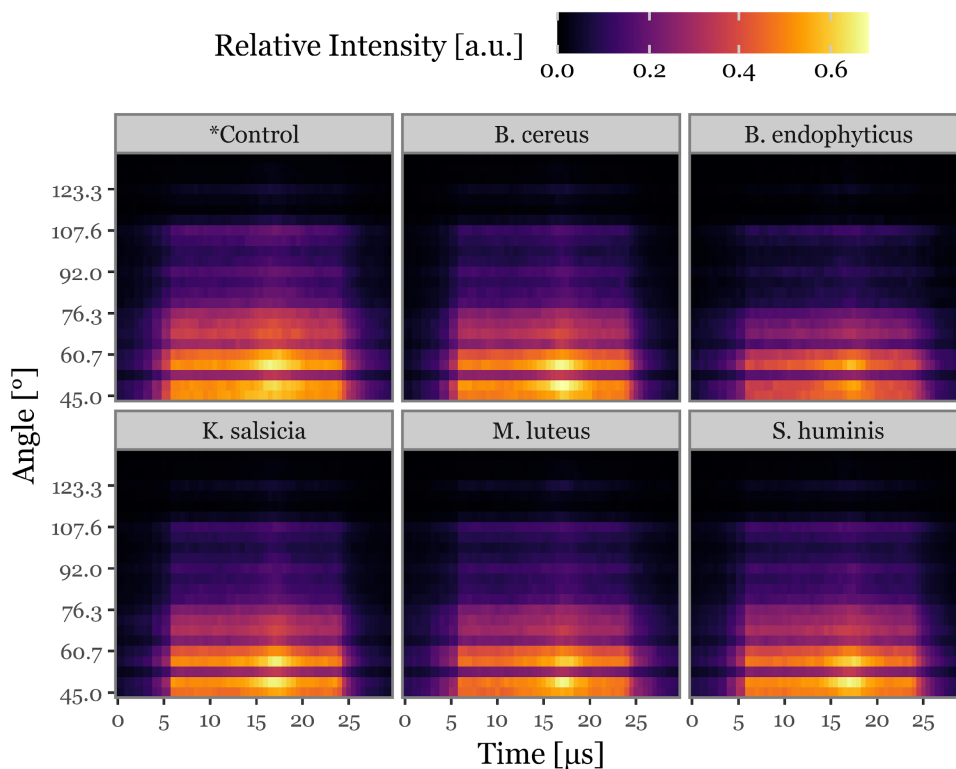


Figure S5. Average scattering images for bacterial aerosols. Heatmaps depicting the average relative light intensity for each combination of timely acquisition (x-axis) and angle (y-axis) and group of aerosolized particles.

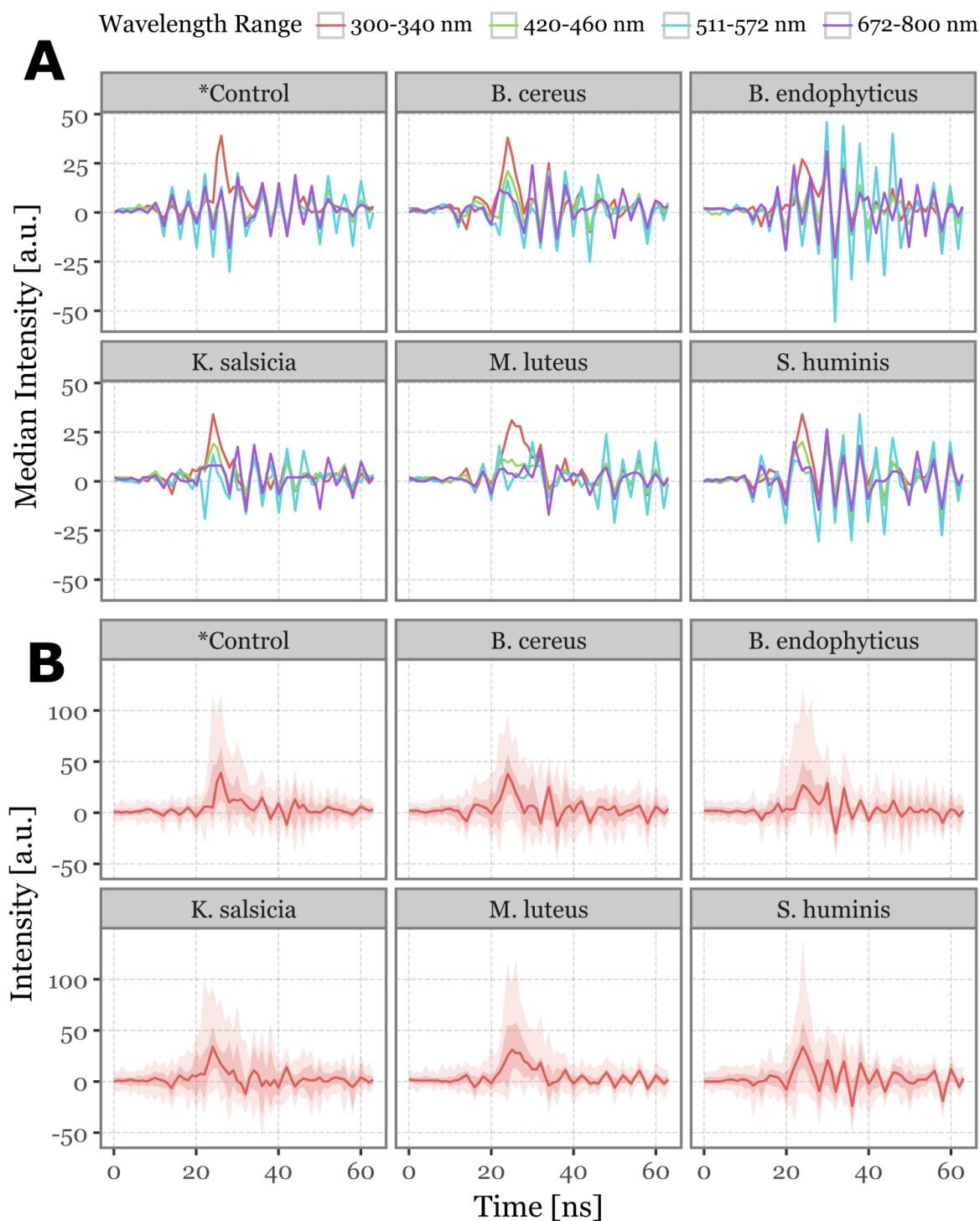


Figure S6. Fluorescence lifetimes for bacterial aerosols. On panel A (top), the median fluorescence intensity as a function of time (in ns) for the 4 specified wavelength ranges across the 100 most fluorescent particles for each of the bacterial groups. On panel B (bottom), the same but focusing only on the 300-340 nm wavelength range, with the dark shaded area representing the interquartile range (25th to 75th percentiles) and the lighter shaded area representing the 5th to 95th percentiles.

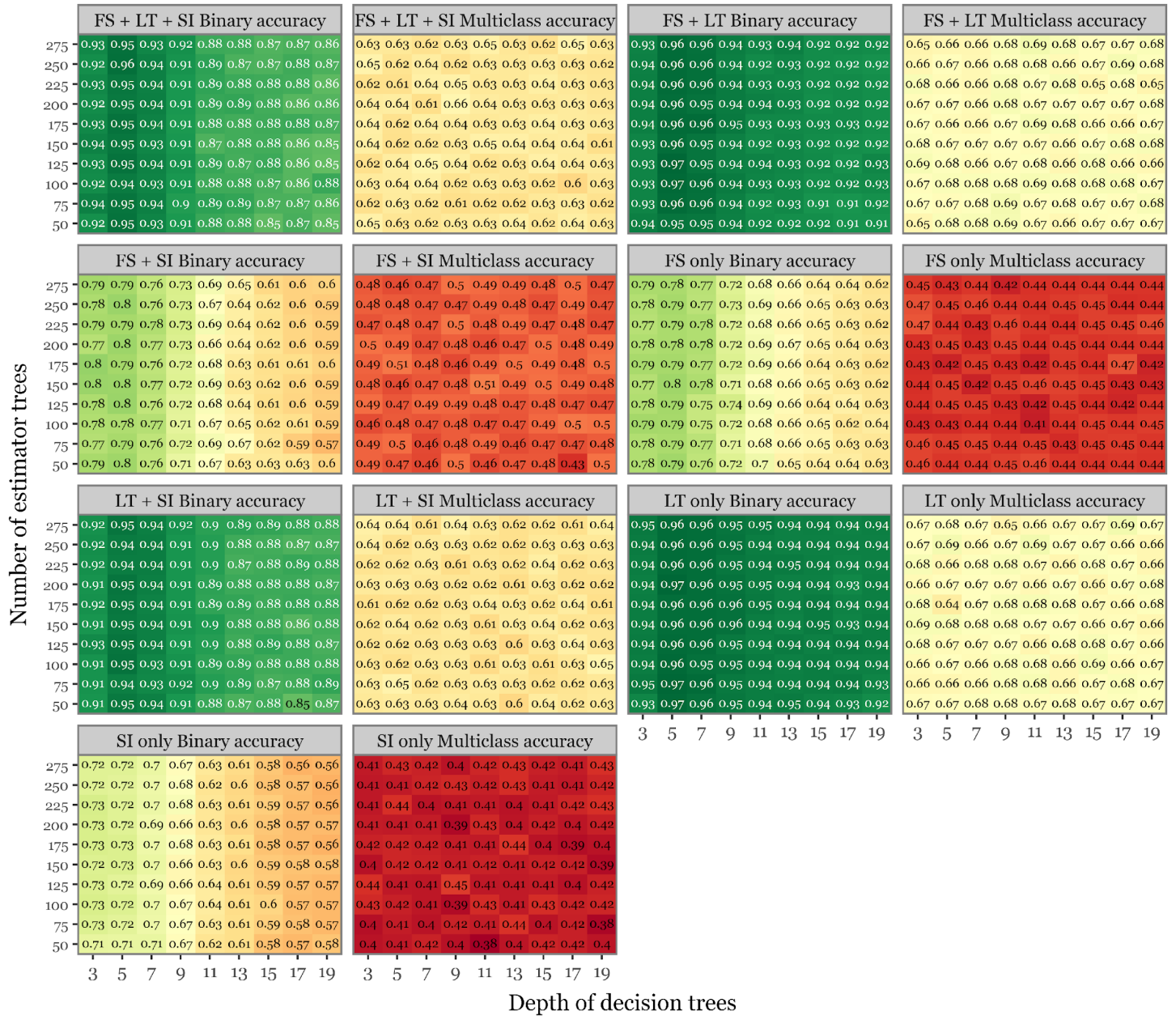


Figure S7. Summary of the hyperparameter optimization process. Each box shows the test set balanced accuracy performance as a function of the depth of decision trees and the number of estimators used on the trained random forest models, both for the binary and multiclass problem (indicated on top of each box). 7 different combinations of predictors are used, also indicated on top (FS=Fluorescence Spectra, LT=Lifetime, SI=Scattering Images).

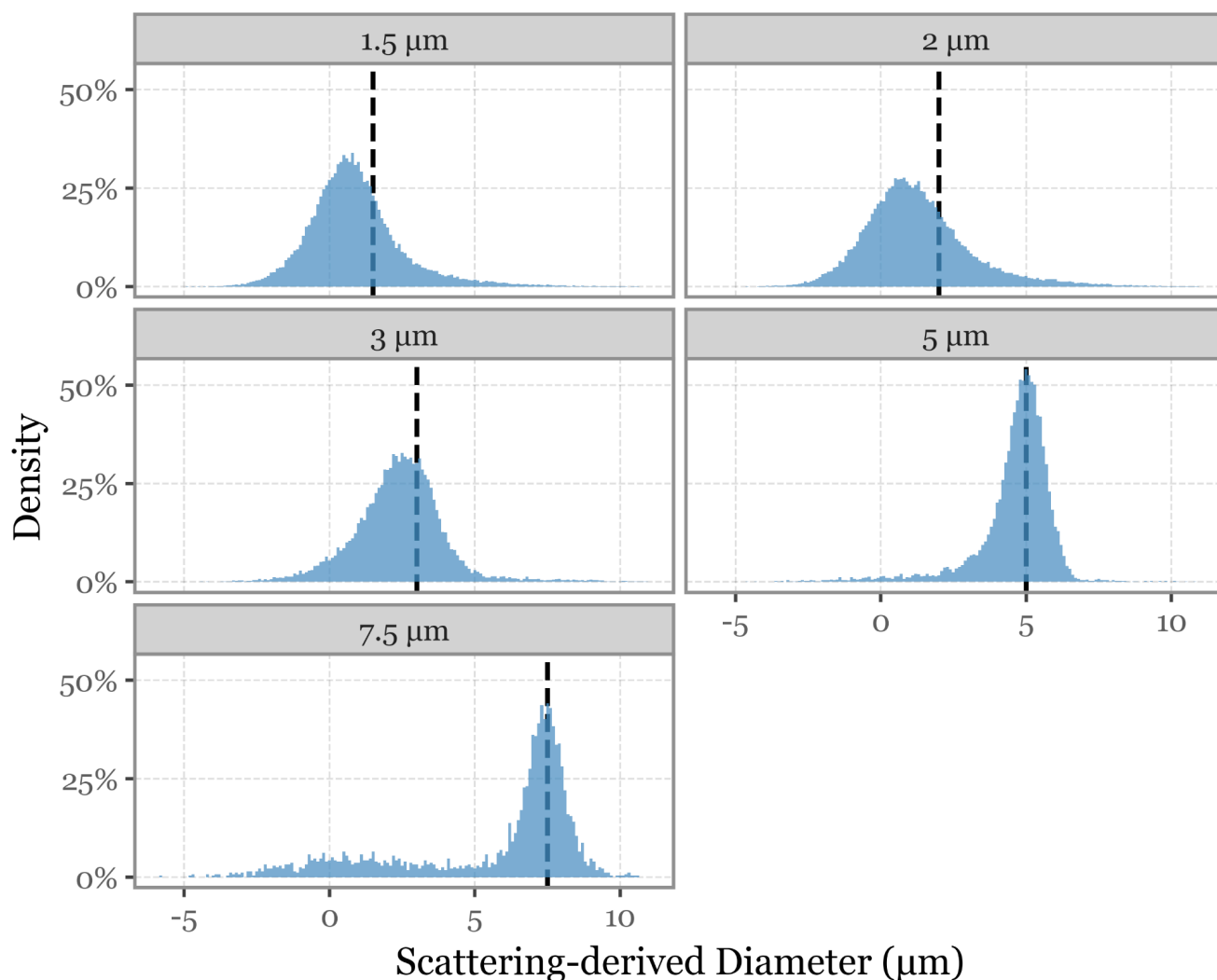


Figure S8. Size distributions of monodisperse particles. Scattering-derived diameters reported by the Rapid-E for aerosolized monodisperse polystyrene microspheres with nominal sizes of 1.5, 2, 3, 5 and 7.5 μm , generated under the same flow and aerosolization conditions as the bacterial experiments. The vertical dashed lines indicate the nominal diameters. Distributions are centered close to the expected values, with only limited right tails and no clear secondary modes, suggesting that the instrument's Mie-based size proxy is stable over the bacterial size range and that large multi-particle aggregates were not frequent under these conditions; small negative estimates arise from noise at very low scattering intensities and are not physically meaningful.